Meteorol. Appl. 6, 11–27 (1999)

Two cases of severe weather in Catalonia (Spain). A diagnostic study

Clemente Ramis, *Grup de Meteorologia, Departament de Física, Universitat de les Illes Balears, 07071 Palma de Mallorca, Spain*

José Manuel López and Joan Arús, *Instituto Nacional de Meteorología, Centre Meteorològic de Catalunya, 08071 Barcelona, Spain*

A diagnostic study of two cases of severe thunderstorms in Catalonia (the north-eastern region of Spain) is presented. The first occurred on 24 August 1993. A squall line, with bow echo configuration in the radar images, crossed Catalonia from west to east. Strong winds, large hail up to 7 cm in diameter, and heavy rain producing floods were observed. The meteorological situation was characterized by an upper-level trough approaching Spain from the north-west. This upper trough developed a low, which displaced the warm, dry air located over the Iberian Peninsula towards the east and north-east. The warm, dry air overran the cold, humid Mediterranean air producing a strong inversion (LID) capped by an elevated mixed layer over the western Mediterranean and also over the Ebro valley. Hand-drawn analyses permitted the identification of a secondary trough; a combination of this trough and a jet streak located over Spain was responsible for the mesoscale lifting mechanism that was able to break the LID and maintain the deep convection. The second case occurred on 31 August 1994. A tornado developed over south Catalonia and large hail, up to 5 cm in diameter, also fell. The meteorological situation was also characterised by an upper-level trough advancing from the west towards Spain. Accurate hand-drawn analyses identified a small thermal low over Catalonia leading to strong convergence at low levels. Over the same area, two jet streaks overlapped their left exit and right entrance zones, producing an enhancement of the ascending motion forced by the low-level convergence. However, the typical environment for supercell development was not present over Catalonia. The tornado was probably produced by a non-supercell thunderstorm.

1. Introduction

Recent observations of severe thunderstorms in Spain (Figure 1), especially in the Mediterranean coastal zones, have increased the interest of Spanish meteorologists in the study of such phenomena. The frequency of severe thunderstorms seems to be higher than that derived from the meteorological archives. As examples we can mention the tornadoes registered in Menorca and Mallorca (Balearic Islands) on 8 October 1992 and 26 October 1991 respectively (Gayá & Soliño, 1993) and on 24 May 1993 in the Guadalajara region (central Spain) (Martín *et al*., 1995). In addition, observations of waterspouts close to the Spanish Mediterranean coast and around the Balearic Islands are not infrequent during late summer and autumn, although their development is not reflected in any meteorological archive or bulletin of hazardous phenomena. Large hail has also been observed in late summer in the vicinity of the Mediterranean coast. For example, hail of more than 6 cm in diameter fell on 15 August 1954 and on 26 August 1968 in Mallorca (Miró-Granada, 1969) or more recently on 15 August 1995 in the Valencia region producing extensive damage (4×10^7 ECUs) to the grape production.

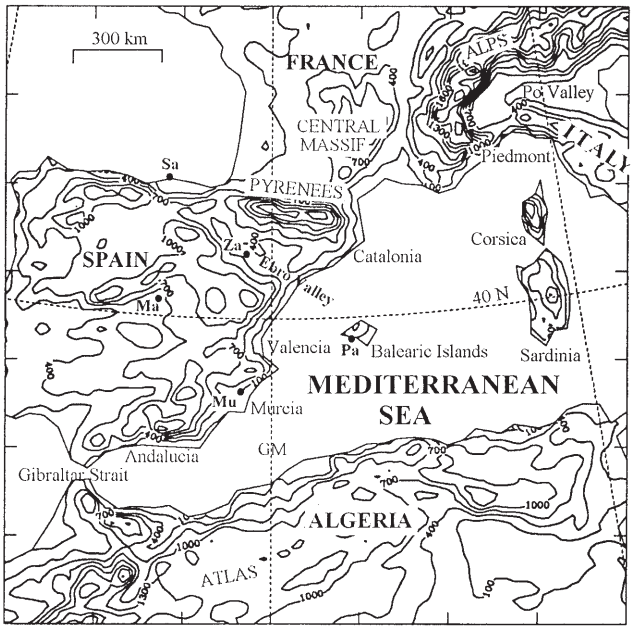

Figure 1. *Map of the western Mediterranean, showing orography and regions referenced in the text. Radiosonde stations used in the study are Sa = Santander, Ma = Madrid, Za = Zaragoza, Mu = Murcia and Pa = Palma de Mallorca.*

Although heavy rain is not considered severe weather by many authors (e.g. Maddox, 1980), the Spanish Mediterranean area is affected during late summer and autumn by very heavy convective precipitation. It represents a climatic characteristic of the region (Font, 1983). These precipitation events can produce floods that result in extensive damage and sometimes loss of life. For this reason a major effort has been to study the meteorological situations in which heavy rain develops. For example, Llasat (1987) provides extensive information on heavy rain events in north-eastern Spain, García-Dana *et al.* (1982), Ramis *et al.* (1994), Ramis *et al.* (1995) present diagnostic studies, and Fernández *et al.* (1995) and Romero *et al.* (1997) describe numerical simulations of heavy rain events in the Spanish Mediterranean region.

Convection organised as a squall line is not very common in south-western Europe and very few studies of such weather events exist. Recently Ducrocq & Bougeault (1995) presented a numerical simulation of a squall line that passed over south-western France. Nearly stationary mesoscale convective systems with circular form are much more frequent and are strongly related to the heavy precipitation occurrences in eastern Spain (Riosalido, 1990).

This paper deals with two cases of severe weather in Catalonia (the north-eastern corner of Spain, Figure 1) that occurred on 24 August 1993 and 31 August 1994. In the former, a squall line, with bow echo in the radar images, crossed Catalonia from west to east producing large hail and heavy rainfall. In the second, a tornado developed in the south of Catalonia, and then produced large hail. Ramis *et al.* (1997) (hereafter referred as RALM) present a description and an observational study of both cases by using satellite, radar, lightning and surface information. Now we present a diagnostic study of both meteorological situations using information available in real time, principally through the McIdas system (Suomi *et al.,* 1983), to the forecasters of the Spanish Instituto Nacional de Meteorología (INM). The information consists of the ECMWF analysis and derived secondary products, as well as SYNOP and TEMP data. Moreover, accurate hand-made analyses, using Meteosat images, complete the diagnostic study to show that small-scale structures can be important in initiating deep convection. These small structures are not well captured by automated products.

The aim of this paper is to expand on the findings of RALM and identify, especially for forecasters, some of the meteorological patterns in which severe weather can appear in south-western Europe. In addition the paper shows the difficulty of issuing an accurate forecast, including nowcasting, in some convective situations.

The paper is organised as follows. The meteorological background for the diagnosis of deep convection is described in section 2. Sections 3 and 4 contain the diagnostic study of the squall line and the tornado cases, respectively. Comments and conclusions are presented in section 5.

2. Meteorological background

The diagnosing and forecasting of severe local storms requires an evaluation of various ingredients and their possible contribution to the development of deep convection. These ingredients are associated with the synoptic scale, which has to produce the favourable environment, and the mesoscale, which provides the lifting mechanisms for low-level parcels (Doswell, 1987). Although convection develops in environments with large spatial and temporal variability (Brooks *et al*., 1994), ingredients on the synoptic scale can be evaluated from operational gridded numerical analyses or forecasts. Known favourable mechanisms are upward vertical motion, water-vapour convergence at low levels and potential or latent instability (Doswell, 1987; McNulty, 1995). The area where these positive mechanisms overlap can be considered as favourable for convective development (Ramis *et al*., 1994).

Quasi-geostrophic theory can be used to determine vertical motion by using the omega equation (Holton, 1993; Hoskins & Pedder, 1980). Water-vapour convergence in a layer close to the ground can be calculated from the flux of specific humidity:

$$F_{\mathrm{W}} = \frac{1}{g}\int_{p}^{p_0} \nabla\cdot(q\,\mathbf{V})\,\mathrm{d}p$$

where q is the specific humidity and $\mathbf{V}$ the horizontal wind. Potential instability for the low troposphere can be determined by means of the difference in equivalent potential temperature between two levels (e.g., 500 and 1000 hPa) and latent instability can be determined by means of the convective available potential energy (CAPE) calculated using each grid point as a sounding. CAPE is calculated from

$$\mathrm{CAPE} = g\int_{\mathrm{LFC}}^{\mathrm{EL}} \frac{\theta-\bar{\theta}}{\bar{\theta}}\,\mathrm{d}z$$

where LFC is the level of free convection, EL the equilibrium level, θ the potential temperature of the rising parcel and $\bar{\theta}$ the potential temperature of the environment. The rising parcel is considered to come from the surface.

Mesoscale mechanisms are much more complex. Their action allows the surface parcels to rise in such a way that they can attain their LFC quickly. Mesoscale mechanisms include physical effects (orographically induced convection), kinematic effects (convergence

lines), mixed orographic-kinematic effects (Ramis *et al*., 1994) and dynamic effects. Among the dynamic effects are ageostrophic motion associated with short-wave troughs or jet streaks at upper levels (Rockwood & Maddox, 1988), interaction between two upper jet streaks (Hakim & Uccellini, 1992), gravity waves (Uccellini, 1975), conditional symmetric instability (Emanuel, 1983) and coupling of upper and lower jet streaks (Uccellini & Johnson, 1979).

In this sense deep convection can be considered a typical example of interaction between scales. The large scale provides the appropriate environment, and mesoscale mechanisms determine when and where convection will develops.

Supercell tornadic storms have been related to environments with high values of CAPE and particular hodographs with strong veering of the wind at low levels (Doswell, 1991; Moller *et al.,* 1994). They have also been associated with high values of environmental storm relative helicity (SRH) in the lowest 3 km (Davies-Jones *et al.,* 1990) and an energy-helicity index (EHI) generally greater than 1 (Davies, 1993). SRH is defined as follows:

$$\mathrm{SRH} = -\int_{z_0}^{z} \mathbf{k} \cdot \left[(\mathbf{V} - \mathbf{c}) \times \frac{\partial \mathbf{V}}{\partial z} \right] \mathrm{d}z$$

where **V** is the horizontal wind, **c** the thunderstorm velocity and **k** the vertical unit vector. If **c** = 0 we have the helicity (H). The EHI has been defined as

$$\mathrm{EHI} = \frac{\mathrm{CAPE} * \mathrm{SRH}}{160000}$$

Supercells normally develop in environments with very high humidity at low levels but with a dry layer at middle levels. This dry layer enhances the downdrafts through the evaporation of the condensation products, occasionally resulting in severe wind gusts (Barnes & Newton, 1986). If the previous conditions are met, a temperature inversion close to the ground is favourable for the development of supercells (Farrel & Carlson, 1989). The inversion inhibits vertical motions and facilitates a high water-vapour content in a layer close to the ground. If some mechanism can break down the inversion, then deep convection can develop. Johns & Doswell (1992) present a review of the techniques for forecasting severe weather and give many references to case studies.

Mid-latitude convection organized as a squall line develops in the warm sector of depressions, often 200–300 km ahead of the surface cold front. The cold front normally has the characteristics of a kata-front. In this situation the warm conveyor belt is overrun by dry, subsiding air from the middle troposphere (Browning, 1986). Dry air, at middle levels, produces strong convective instability. Meteorological conditions associated with bow echoes over the United States have been studied by, among others, Johns & Hirt (1987), Johns (1993) and Przybylinski (1995). Johns & Hirt (1987) indicate that a family of downburst clusters from convective cells produces bow echoes. When the area affected by the convectively induced winds has an elliptic form with a major axis of at least 400 km and the wind gusts are greater than 50 kn, with other complementary criteria, the event is called a '*derecho*'. Johns & Hirt (1987) identified two basic patterns: progressive and serial. The progressive case, which develops mainly during the warm season, has been associated with relatively weak synoptic-scale features with westerly or north-westerly winds at mid- and upper-tropospheric levels. The serial case, which occurs in all seasons, appears in a synoptic pattern characterized by a strong, migrating low-pressure system, and the squall line develops along or ahead of the cold front.

As we will show below, the two cases presented in this paper include many of the indicated ingredients. Diagnosis has been conducted in two steps. In the first we identify large areas where there is a high potential for convective development. In the second we identify mesoscale mechanisms that, acting in the previously identified broad area, are able to develop convection. As indicated in Rockwood & Maddox (1988), this is frequently a very difficult task.

3. The squall line case (24 August 1993)

3.1. The event

RALM describe in detail the meteorological event. Early in the afternoon, convection developed over the Mediterranean Sea, affecting the coastal zone and producing heavy rain over south Catalonia. Late in the evening, large hail, up to 7 cm in diameter, fell in central and eastern Catalonia as well as heavy flood-producing rain. At the same time strong north-westerly winds, with gusts up to 20 m s^{-1}, occurred. Temperature, humidity and pressure changed very quickly with the pass of the convection (see Figures 3 and 4 in RALM). Radar images show a convective line with multicellular structure and bow echo configuration that moved from west to east at 40–50 km h^{-1} (see Figure 6 in RALM). Meteosat images also show a mesoscale convective system that developed west of Catalonia and moved towards the east (see Figure 5 in RALM).

3.2. Synoptic-scale overview

The large-scale situation on 24 August 1993 at 1200 UTC is characterized at low levels (Figure 2(*a*)) by an anticyclone located to the west of the British Islands

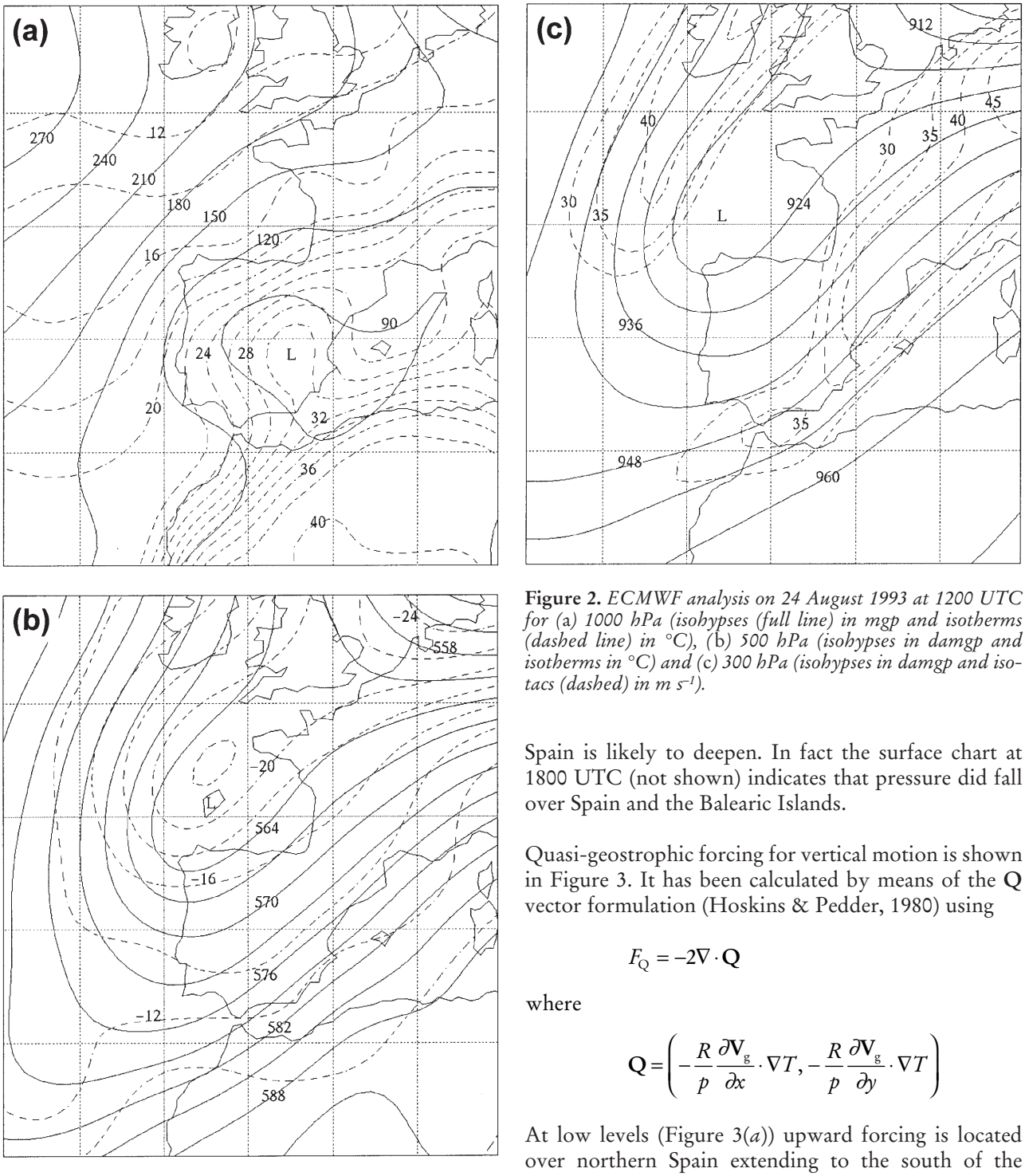

Figure 2. *ECMWF analysis on 24 August 1993 at 1200 UTC for* (a) *1000 hPa (isohypses (full line) in mgp and isotherms (dashed line) in °C),* (b) *500 hPa (isohypses in damgp and isotherms in °C) and* (c) *300 hPa (isohypses in damgp and isotacs (dashed) in m s^{-1}).*

and a low-pressure centre over Spain where the pressure gradient is very weak. A cold front is located over western Spain extending toward northern Italy and moves slowly from the north-west (see Figure 5 in RALM). At upper levels, 500 and 300 hPa (Figure 2(*b*) and (*c*)), a trough, positively tilted, is located from the English Channel towards north-west Spain. At 300 hPa there is a jet streak in the descending part of the trough and another jet is located in its ascending part over the Spanish Mediterranean coast. The vertical axis of the trough is tilted towards the north-west, indicating that the wave is under development and that the low over Spain is likely to deepen. In fact the surface chart at 1800 UTC (not shown) indicates that pressure did fall over Spain and the Balearic Islands.

Quasi-geostrophic forcing for vertical motion is shown in Figure 3. It has been calculated by means of the **Q** vector formulation (Hoskins & Pedder, 1980) using

$$F_{\mathrm{Q}} = -2\nabla \cdot \mathbf{Q}$$

where

$$\mathbf{Q} = \left(-\frac{R}{p}\frac{\partial \mathbf{V}_{\mathrm{g}}}{\partial x} \cdot \nabla T, -\frac{R}{p}\frac{\partial \mathbf{V}_{\mathrm{g}}}{\partial y} \cdot \nabla T \right)$$

At low levels (Figure 3(*a*)) upward forcing is located over northern Spain extending to the south of the Balearic Islands, while at 500 hPa (Figure 3(*b*)) major upward forcing is located just ahead of the trough, although small values occur over Catalonia. Relative humidity at the surface (Figure 4) is very high over the Spanish Mediterranean coast as well as in the Ebro valley (see Figure 1 for location). This indicates the presence of convective instability in the 1000–500 hPa layer over most of the western Mediterranean and the eastern part of Spain. Convergence of water vapour also exists in the 1000–850 hPa layer along the Spanish Mediterranean coast (not shown).

It is known that the vertical motion does not match exactly the sign of the vertical forcing at low levels

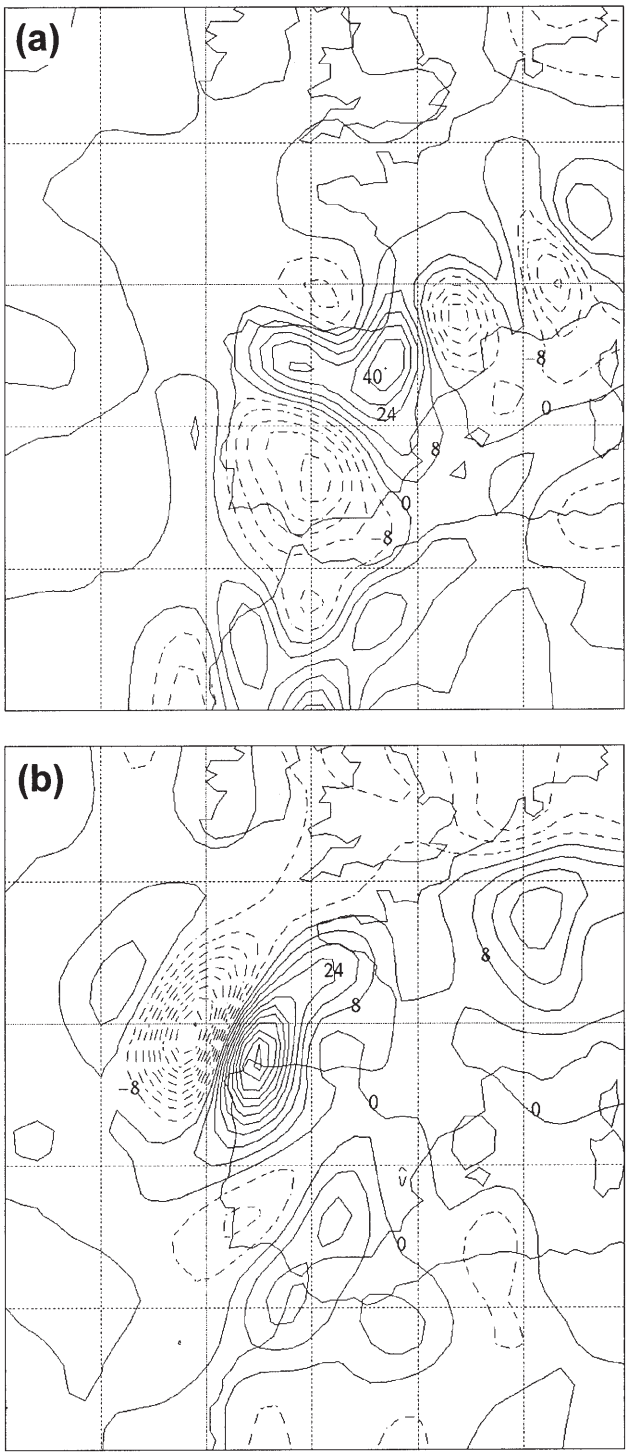

Figure 3. *Quasi-geostrophic vertical forcing (unit 10^{-18} m kg^{-1} s^{-1}) on 24 August 1993 at 1200 UTC, deduced from ECMWF analyses, for* (a) *925 hPa and* (b) *500 hPa. Positive values (full line) indicate upward forcing.*

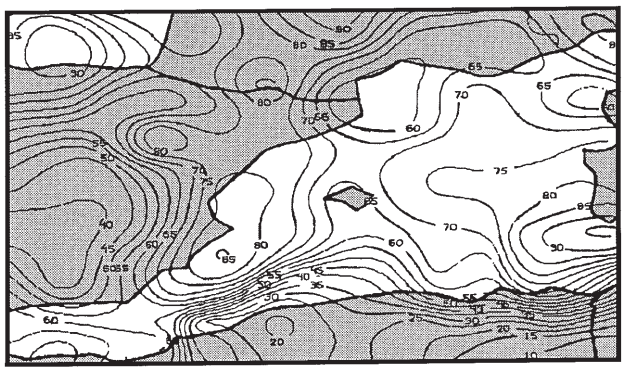

Figure 4. *Relative humidity (INM analysis) at the surface on 24 August 1993 at 1200 UTC.*

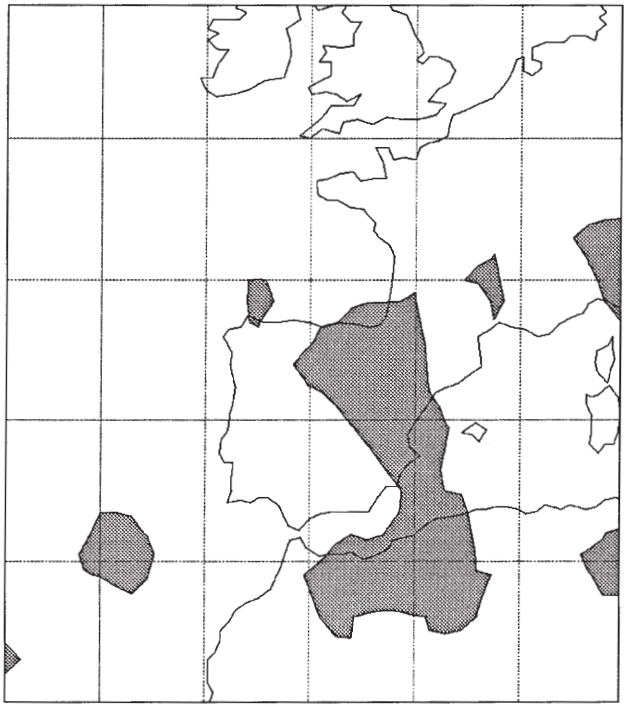

Figure 5. *Composite chart on 24 August 1993 at 1200 UTC deduced from ECMWF analyses. Shaded zones indicate overlap of quasi-geostrophic upward forcing at 850 hPa, convergence of water vapour in the 1000–850 hPa layer and convective instability between 1000 and 500 hPa.*

(Durran & Snellman, 1987; Ramis & Alonso, 1992), as consequence of the elliptic character of the omega equation. The inversion of the Laplacian operator yields a vertical motion field smoother than the forcing. At the same time, the derived vertical motion depends strongly on the boundary conditions, especially the bottom boundary condition if the orography-induced vertical motion is included. However, if the forcing is positive at low levels, the vertical motion will be upward if there is not negative forcing at upper levels. In this sense, a composite chart showing where there is overlap between low-level upward forcing, convective instability and low-level moisture convergence can indicate where the large-scale situation favours the development of convection. Figure 5 shows such a composite chart. The favourable area includes most of the eastern Spain and south-west of the Balearic Islands.

In this synoptic scenario, there are significant differences in the vertical structure of the atmosphere over the Mediterranean and mainland Spain. Figure 6 shows soundings at Palma, Zaragoza and Madrid (see Figure 1

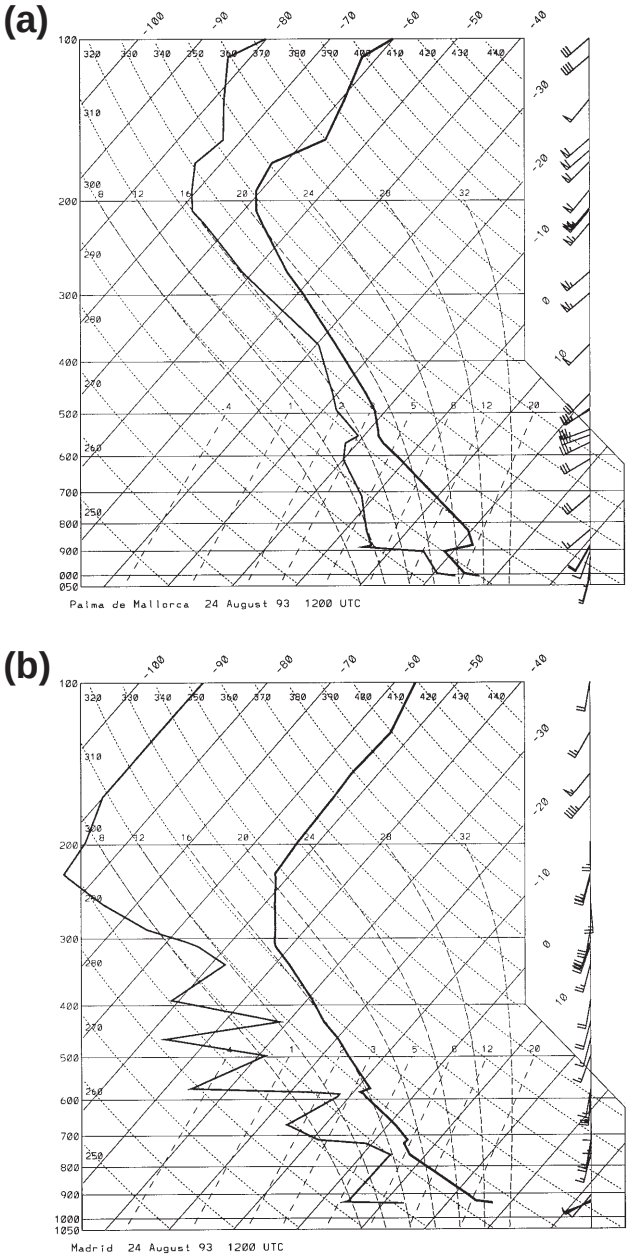

Figure 6. *Radiosounding on 24 August 1993 at 1200 UTC for* (a) *Palma,* (b) *Madrid and* (c) *Zaragoza.*

for location) at 1200 UTC. The sounding from Palma (Figure 6(*a*)) shows a very humid low layer capped by an inversion, above which there is a dry layer with a quasi-adiabatic lapse rate and increasing relative humidity. Instability for low-level parcels can be very strong if they can break the inversion as indicated by the value (–9) of the lifted index (Galway, 1956) and by the CAPE value, which is 4400 J kg^{-1}. This structure meets the conditions of an elevated mixed-layer inversion known as a LID (Farrell & Carlson, 1989). The wind is weak at low levels and the vertical shear is small and indicates warm-air advection. The atmospheric vertical structure over Murcia (not shown, see Figure 1 for location) is very similar to that of Palma. Instability is very high for the parcels that can break the inversion. The lifted index is –7 and the CAPE is 3939 J kg^{-1}. The low-level winds and vertical shear are stronger than in Palma, and there is a maximum at 800 hPa. At the centre of Spain, in Madrid (Figure 6(*b*)), the sounding shows very different characteristics. A deep low layer has an adiabatic lapse rate as a consequence of the strong radiative heating. Although the surface parcels are much dryer than in the Mediterranean area, instability is notable because of the high lapse rate. The lifted index is –7 and CAPE is 1399 J kg^{-1}. The wind is very weak and the vertical shear shows cold advection. The Zaragoza sounding (Figure 6(*c*)) shows similar low-level characteristics to the soundings from Palma and Murcia. Instability is not as strong as over the Mediterranean with a lifted index value of 2 although the total total's index (Miller, 1972) attains a value of 49. CAPE for the lower parcel is 0. A dry layer at 400 hPa can be identified. The wind and vertical shear are very weak at low levels, but a jet streak is present at upper levels. The Santander sounding (not shown, see Figure 1 for location) does not show any significant characteristic feature at low levels; it is representative of the cold air mass located over the Cantabrian sea.

The LID has been identified as a major ingredient for the development of severe convection in the United States (Benjamin & Carlson, 1986; Farrel & Carlson, 1989). As the LID appears to play an important role in the development of the severe convection, it is interesting to discuss how it formed. For this, it is necessary to consider the evolution of the synoptic situation.

As a consequence of the intense solar heating, a thermal low was located over the Iberian peninsula, as is normal in August (Font, 1983). The air associated with the thermal low was very dry and resulted in a super-adiabatic lapse rate (Alonso *et al.*, 1994). In this situation, coastal Mediterranean zones develop sea-breeze circulations that produce an influx of humid and cold air inland from the Mediterranean. This intrusion travels a

great distance into the Ebro valley (see Figure 1 for location) as far as Zaragoza (Millán & Artiñano, 1992), but it is stopped by the orography along the rest of the coast, as confirmed by Figure 4. In this situation, when the synoptic perturbation arrives at the Iberian peninsula with a well-marked trough at upper levels, pressure deepens over Spain and forms a low that displaces the dry and warm air towards the east and north-east. This dry, warm air overruns the humid, relatively cold Mediterranean air forming the LID. Its formation is favoured by the sea breezes along the eastern coast of Spain where radiation is high. Note that the potential temperature at the top of the inversion in Palma coincides with the potential temperature at the surface in Madrid.

The strength of the LID (its ability to suppress convection) can be defined according to Farrel & Carlson (1989) as

$$\delta = \theta_{sw1} - \theta_{wb}$$

where θ_{sw1} is the saturation wet-bulb potential temperature at the base of the elevated mixed layer (the top of the inversion) and θ_{wb} the surface wet-bulb potential temperature. Figure 7 shows the LID analysis on 24 August 1994 at 1200 UTC. Orography (see Figure 1) has been considered when drawing the δ-isolines as well as the values of δ deduced from the radiosonde data. The edge of the LID also can be identified with the spatial distribution of the relative humidity at the surface (Figure 4). There is humid air inland in the Ebro Valley, but the air north-west of Zaragoza is dryer, showing the end of the moist Mediterranean air.

The synoptic study shows that although there are ingredients for deep convection over the Mediterranean

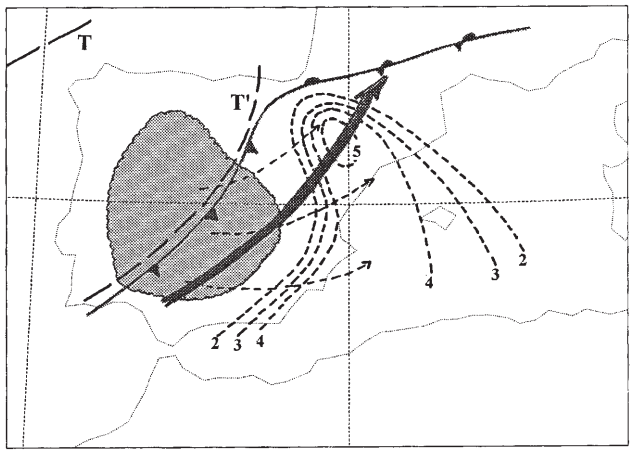

Figure 7. *Hand-drawn composite chart showing δ isolines of the LID (dashed lines), surface fronts, trough axis at 500 hPa (T and T') and jet streak at 300 hPa on 24 August 1993 at 1200 UTC. The shaded zone represents the area where upper mixed layer formed and dashed arrows represent the displacement of the warm and dry air that formed the LID overrunning the Mediterranean air.*

Spanish coast and the Ebro valley, the inversion inhibits vertical motion from low levels. In this situation, if convection develops after breaking the LID, it will be deep. It is necessary, therefore, to look for sufficient large mesoscale forcings that permit the low-level parcels to break through the LID.

3.3. Mesoscale study

Hand-drawn reanalysis of isobaric surfaces can help reveal mechanisms for triggering convection, and to distinguish between the different characteristics of the early afternoon and the evening convection that affected Catalonia.

Figure 8 shows the reanalysis at 850, 500 and 300 hPa on 24 August 1993 at 1200 UTC. At 850 hPa warm advection is evident over north-eastern Spain. At 500 and 300 hPa a secondary trough can be identified over Spain, as indicated by winds and temperatures over Lisbon and Madrid. The Meteosat water-vapour image (Figure 9) at 1200 UTC helps identify the trough and locate more accurately the jet streak over Spain (compare Figures 2(*c*) and 8(*c*)) It is likely that this secondary trough produced the forcing for developing the shallow convection over central Spain ahead of the cold front (see Figure 5 in RALM), where the low-level humidity is very low. The differential temperature advection between low and upper levels (see Figures 8(*a*) and (*b*)) probably led to further destabilization over the head of the Ebro valley as the secondary trough moved towards the north-east.

At 1200 UTC the most important convection was located over the Mediterranean, close to the coast of Catalonia (see Figure 9, and Figure 5 in RALM). The convective cell that affected the Catalonian coast in the early afternoon developed close to Valencia (see Figure 1 for location). The lifting mechanism for these convective storms was probably the 850 hPa convergence that appears in that area. This convergence should be associated with the low-level jet that existed over Murcia and the flux from the north, which was related to the descending part of the ridge located over eastern Spain. Figure 10 shows the surface mesoscale analysis at 1200 UTC where a conceptual model of pressure distribution around a thunderstorm (Schofield & Purdom, 1986) has been combined with Meteosat images because of the lack of data over the sea. Moist inflow for the thunderstorm complex was provided by the winds from the north-east. With a LID strength of about 4 °C, vertical motions forced by convergence can start over the LID in the quasi-adiabatic layer. The LID could then be broken by the convective currents and the humid air, close to the ground, incorporated in the convective cell. Buzzi *et al.* (1991) show that convection initialized at medium levels with an inversion close to the ground can produce this effect. Further, convection was driven towards the north-east by the winds at

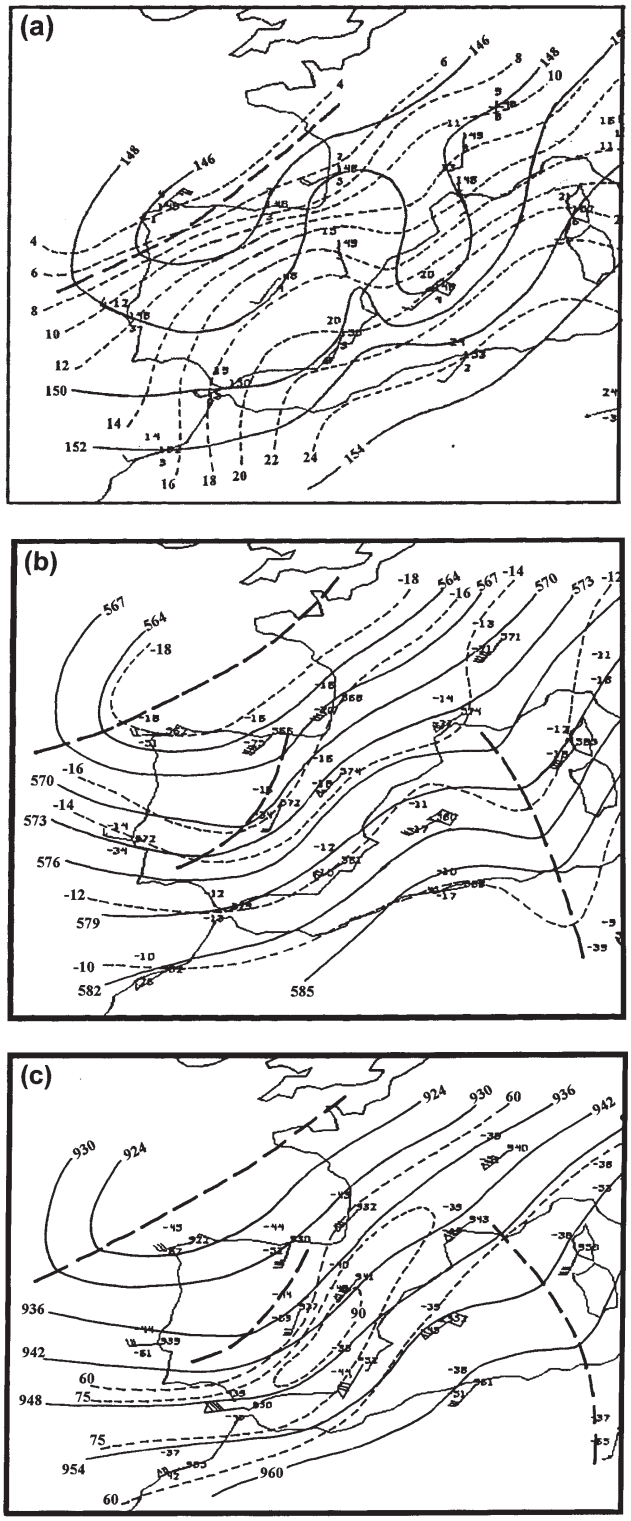

Figure 8. *Hand-drawn analysis on 24 August 1993 at 1200 UTC for* (a) *850 hPa (isohypses (full line) in damgp, isotherms (dashed) in °C),* (b) *500 hPa (isohypses in damgp, isotherms in °C) and* (c) *300 hPa (isohypses in damgp, isotachs (dashed) in kn).*

upper levels. The circular aspect of the thunderstorm as seen in the Meteosat image (see Figure 9, and Figure 5 in RALM) demonstrate that the cell is not affected by strong upper-level winds, confirming the position over Spain of the jet streak in the 300 hPa hand analysis.

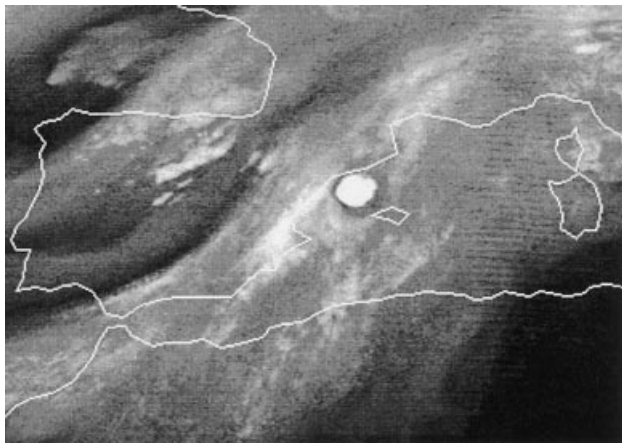

Figure 9. *Meteosat water-vapour image on 24 August 1993 at 1200 UTC.*

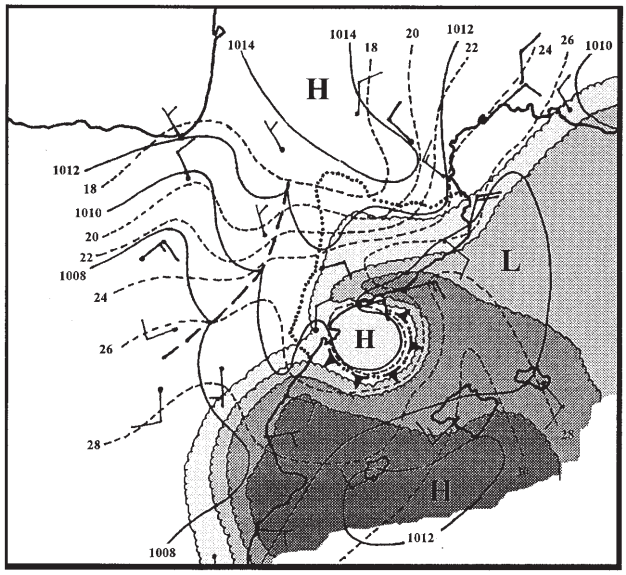

Figure 10. *Mesoscale hand-drawn surface analyses on 24 August 1993 at 1200 UTC. Full line: isobars. Dashed lines: isotherms. Scallopped lines and shaded regions represent zones where the dew point is higher than 18, 20, 22 and 24 °C. Winds are plotted following the conventional synoptic rules. The dotted line represents Catalonia's border.*

As indicated in RALM, the convective line located at 1200 UTC in central Spain moved to the west of Catalonia by 1500 UTC (see Figure 5 in RALM). In our opinion, deep convection occurred in response to the vertical ageostrophic circulation associated with the secondary trough and the left exit of the jet streak when both systems approached. The associated vertical motion was large enough to destroy the LID and then allow the deep convection to form. In that area the strength of the LID is 2 °C (see Figure 7). Similar breaks in such a relatively weak LID have been observed previously (Farrell & Carlson, 1989). The secondary trough can provide dry air at medium levels when it moves with the thunderstorms. Figure 11 shows the descending motion caused by the secondary

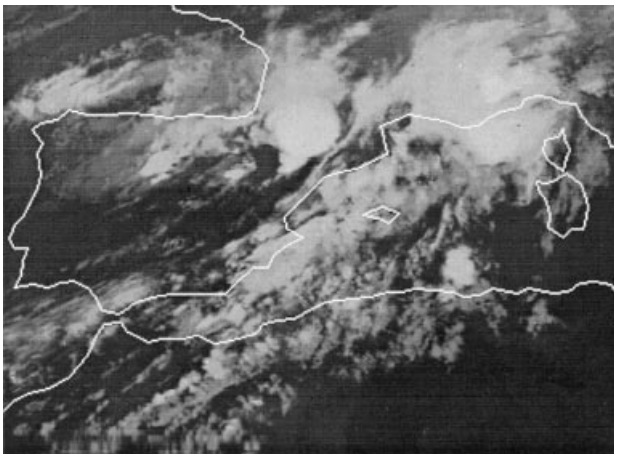

Figure 11. *Meteosat infrared image on 24 August 1993 at 1800 UTC.*

trough, which was to the rear of the convective cells. The triangular shape of the convective cloud tops demonstrates that they were affected by the jet streak over eastern Spain.

After 1500 UTC, the convective cells moved eastwards, to the right of the wind at upper levels. This rightward deviation is very common in severe thunderstorms (Weisman & Klemp, 1986). In this case it seems that thunderstorms moved towards the area with high humidity at low levels, which is to the right of the upper-level winds.

The vertical motion can also be obtained trough the irrotational part of the ageostrophic flow deduced from ECMWF gridded data. We have used the technique described by Endlich (1978) to separate the ageostrophic wind into its irrotational and non-divergent components. Figure 12 shows that at low levels (925 hPa) there is a convergence line over the Mediterranean Spanish coast but the convergence is especially strong west of Catalonia. At upper levels (300 hPa) divergence is strong over the same area. This is further evidence that ageostrophic synoptic-scale vertical motions helped to weaken the LID and facilitated the action of the mesoscale mechanisms.

The organization of the convection as a squall line is favoured if the cold front is a kata-front (Browning, 1986). This frontal character has been investigated through cross-sections (not shown) of the wet-bulb potential temperature (θ_w) and the thermal frontal parameter (*TFP*), as defined by

$$TFP = -\frac{\nabla\theta}{|\nabla\theta|} \cdot \nabla |\nabla\theta|$$

where θ is the potential temperature. The kata character of the front is not well represented but some evidence can be inferred from the form of the *TFP* and θ_w isolines. In particular, the cross-section of θ_w shows that the isotherms form a nose aloft over the location of the surface front. It seems clearer that the dry air at middle levels is associated with the secondary trough, as indicated in the Meteosat image (Figure 11).

The surface-pressure field associated with the squall line can be constructed by using surface observations and traces of meteorological parameters. Figure 13 shows the surface-pressure analyses at 1800 UTC and 2100 UTC. Radar images (see Figure 6 in RALM) have been used to locate the convective line. The pressure trace at l'Estartit (see Figure 4 in RALM) has been considered conservative in time and integrated into the surface observations. The high pressure associated with the squall line appears embedded within the general cyclonic circulation over Spain and the western Mediterranean.

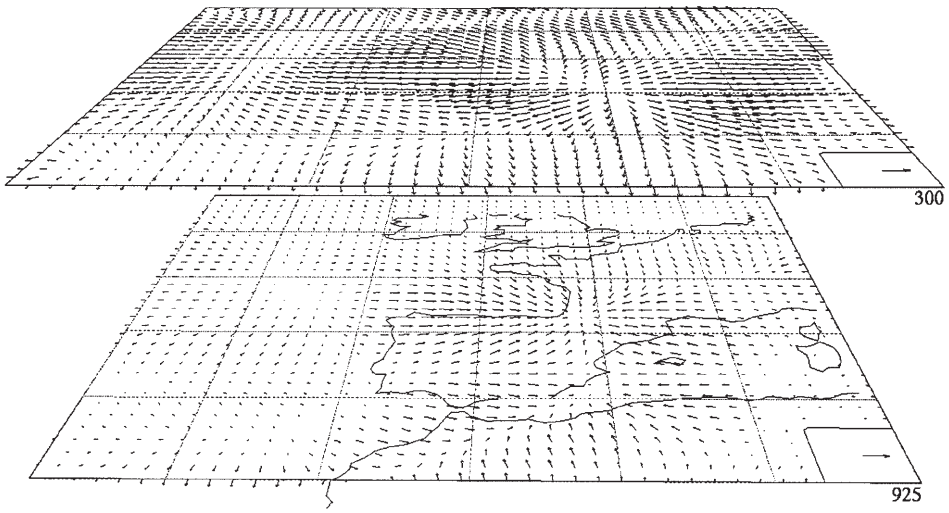

Figure 12. *Irrotational part of the ageostrophic wind at 925 and 300 hPa on 24 August 1993 at 1200 UTC. Arrow in the right corner represents 5 m s^{-1}.*

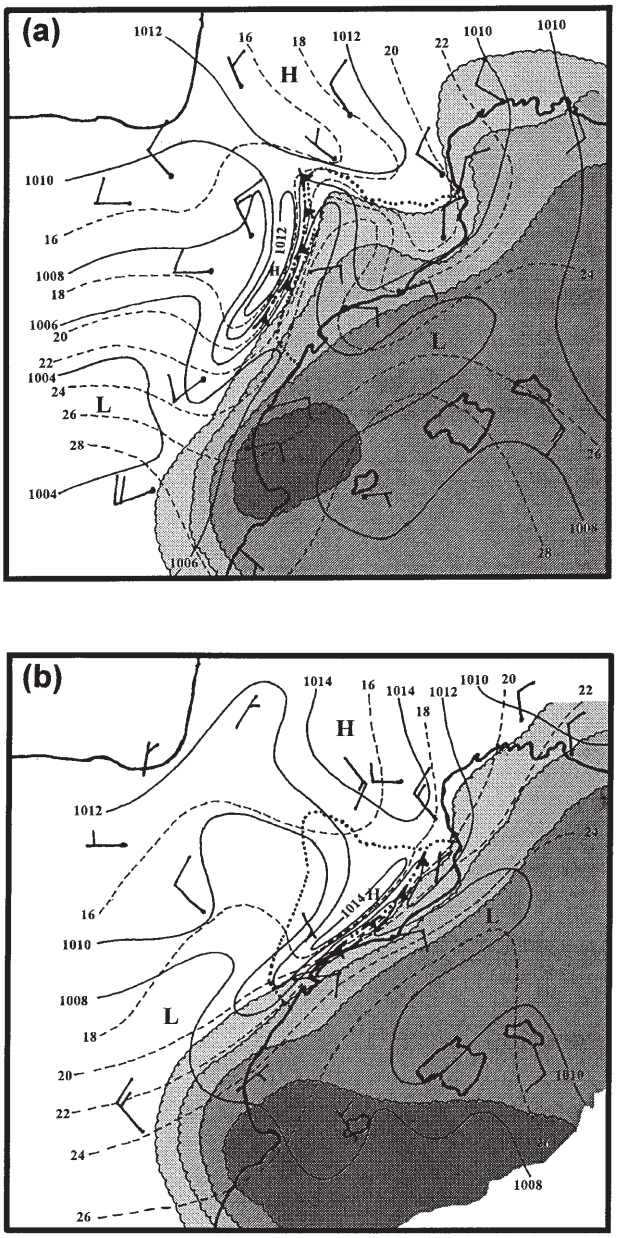

Figure 13. *Mesoscale hand-drawn surface analyses at* (a) *1800 UTC and* (b) *2100 UTC on 24 August 1993. Isopleths and shading as in Figure 10.*

4. The tornado case (31 August 1994)

4.1. The event

Although a detailed description is included in RALM, we also present a short summary for completeness. At about 14.30 UTC a tornado developed over south Catalonia. Its intensity was estimated as F1 with intervals of F2 on the Fujita scale (Fujita, 1989). Moreover, hail, up to 6 cm in diameter, was observed. Meteosat images show that convection over Catalonia developed in an explosive form over an area completely free of clouds. After the development of the tornado, a very clear V-shape signature (McCann, 1981) was observed on a NOAA image. Radar images show that the tornado developed when two convective cells merged, but no supercell signatures, such as hook echoes, can be identified.

4.2. Synoptic overview

At 1200 UTC there was a surface low located over north-west France with a weak eastward moving cold front which extends to the south through Spain (Figure 14(*a*)). A secondary low was located over Spain. Both structures can be clearly identified on the Meteosat image at 1200 UTC (see Figure 10 in RALM). At 850 hPa (not shown) the low presents a very weak circulation but the front is well marked by the isotherms. Over eastern Spain the cyclonic circulation is very weak. At upper levels, 500 and 200 hPa (Figures 14(*b*) and 14(*c*)), a trough with a north–south axis over Spain produces a south-west flux over the Spanish Mediterranean coast. A thermal trough at 500 hPa is also identified over Spain and the western Mediterranean. At 200 hPa, jet streaks can be identified both in the descending and ascending parts of the trough, as well as a subtropical jet streak over the western Mediterranean. At the same time the surface air over the Mediterranean is very humid, while the air to the west of Catalonia is dry, as shown by the distribution of the wet-bulb potential temperature at 1000 hPa (Figure 15). This figure indicates that over eastern Spain there is a boundary between two air masses of different water-vapour content.

Quasi-geostrophic forcing of vertical motion shows that there is upward forcing over Catalonia at low levels (925 hPa, Figure 16(*a*)) while at medium levels (500 hPa) the forcing is downward (Figure 16(*b*)). At 500 hPa the major upward forcing is located to the east of the trough. Convective instability is very high over the western Mediterranean and eastern Spain and water-vapour convergence in the layer 1000–850 hPa is restricted to the western Mediterranean and north-eastern Spain. Figure 17 shows the area where upward quasi-geostrophic forcing at 850 hPa, convective instability and water-vapour convergence at low levels overlap. As can be seen, the three mechanisms become favourable over Catalonia.

The vertical structure of the atmosphere over Catalonia has to be inferred from the soundings of Palma de Mallorca and Zaragoza, as well as using observations made in Catalonia. At 1200 UTC over Palma (Figure 18(*a*)), although there is a stable layer close to the ground, the instability is strong, since CAPE attains values of 2740 J kg^{-1} and the convective energy inhibition reaches 110 J kg^{-1}. A dry layer is present between 700 and 500 hPa. The wind is from the south-west with a very small vertical shear, so the helicity just attains 20 m^2 s^{-2}, indicating a weak integrated warm advection in a layer between the surface and 3 km (Tudurí & Ramis, 1997). Stability indices also show that instability is important since the lifted index is –8 and total total's index is 50. Over Zaragoza (Figure 18(*b*)),

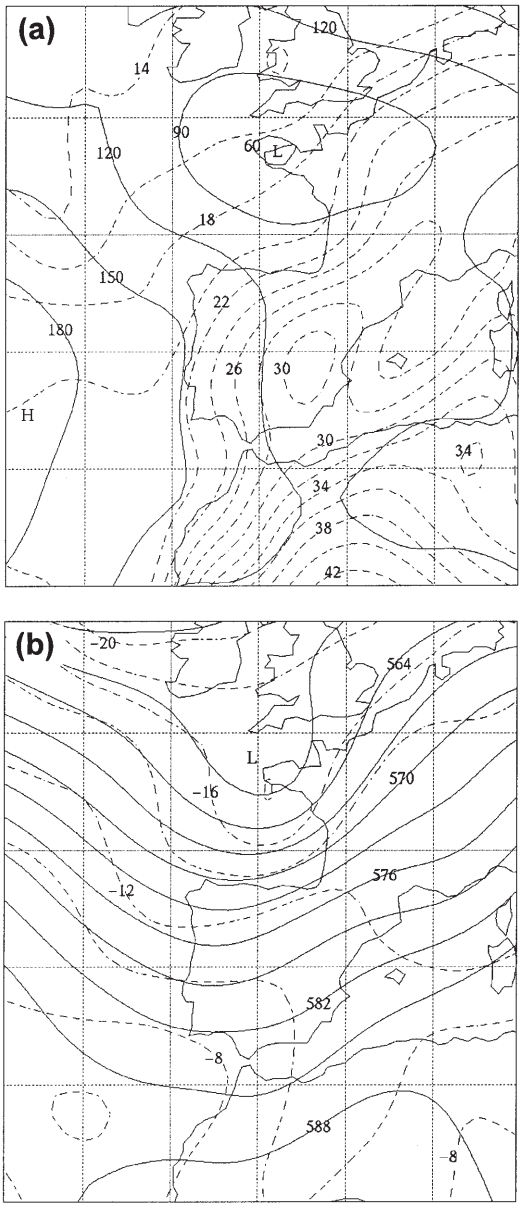

Figure 14. *ECMWF analyses on 31 August 1994 at 1200 UTC for* (a) *1000 hPa (isohypses (full line) in mgp and isotherms (dashed) in °C),* (b) *500 hPa (isohypses in damgp and isotherms in °C) and* (c) *200 hPa (isohypses in damgp and isotachs (dashed) in m s^{-1}).*

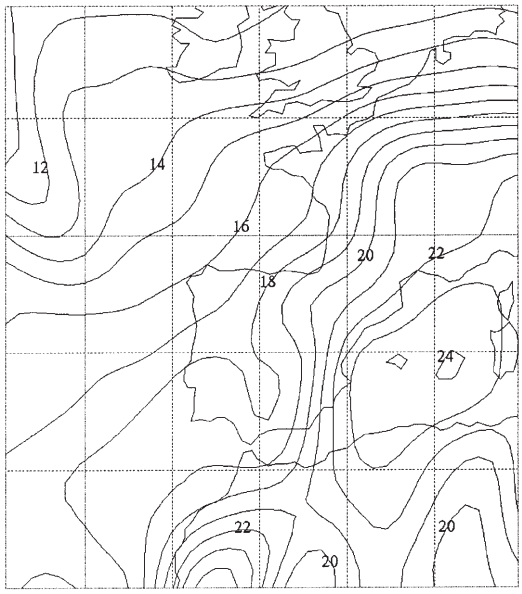

Figure 15. *Wet-bulb potential temperature (°C) for 1000 hPa on 31 August 1994 at 1200 UTC deduced from ECMWF data.*

although the surface layer is less stable than over Palma, the total instability is much weaker, since CAPE is 1016 J kg^{-1} and convective energy inhibition is 193 J kg^{-1}. The environment is dry above 750 hPa throughout the troposphere. The wind is from the south-west, also with a very weak vertical shear. The helicity is –5 m^2 s^{-2}, which indicates cold advection. Stability indices show the same possibility of convection since the lifted index is –3 and total total's index is 49. Approximate spatial distribution of CAPE and helicity can be inferred from the ECMWF gridded data, using each grid point as a sounding. Figure 19 shows such distributions on 31 August 1994 at 1200 UTC. Helicity is positive over the western Mediterranean and Spanish Mediterranean coast but negative over much of the Iberian peninsula. There are large values of CAPE over the Balearic islands extending to the Spanish coast. It is clearly depicted that the CAPE and helicity values over the Balearic islands and Zaragoza are quite similar to those obtained directly using the sounding data. If one looks at Figure 19 and the weather maps, it appears that the vertical structure over Mallorca is representative of the environment over Catalonia.

In conclusion, synoptic-scale ingredients over Catalonia are favourable for convection. Moreover, dry air exists at medium levels, which is favourable for severe storms. It is much more difficult to determine whether the environment is favourable for supercell development. As shown in RALM, the convection developed over Catalonia was almost stationary, and so

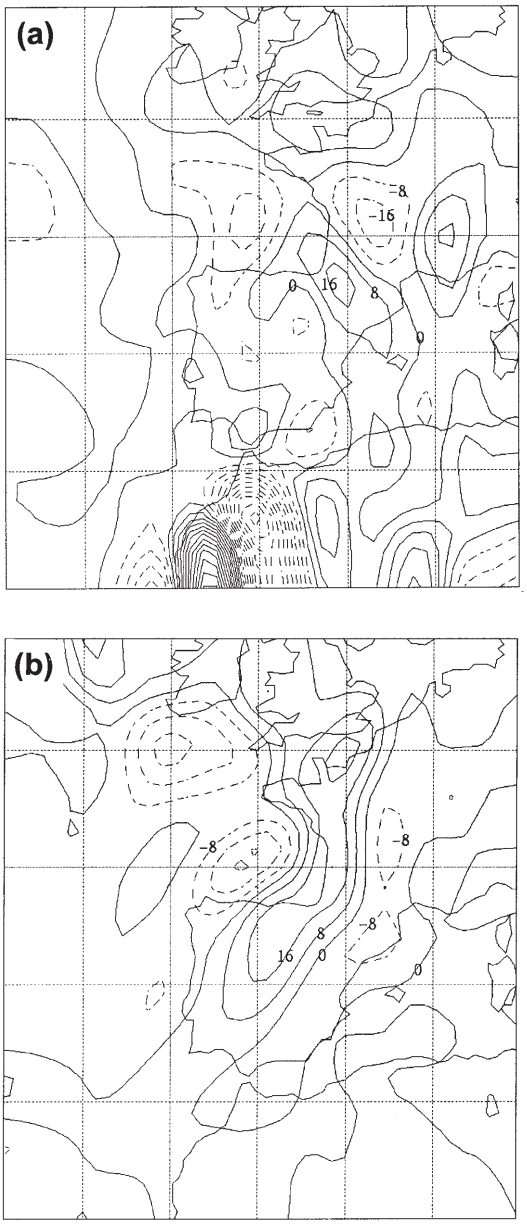

Figure 16. *Quasi-geostrophic vertical forcing (unit 10^{-18} m kg^{-1} s^{-1}) on 31 August 1994 at 1200 UTC, deduced from ECMWF analyses, for* (a) *925 hPa and* (b) *500 hPa. Positive values (full line) indicate upward forcing.*

the helicity can be considered representative of the storm relative helicity. We have seen that the helicity is weak and, although CAPE is large, the EHI is less than 1. It seems that the environment does not match those widely associated with the supercell development.

As indicated in RALM, signatures available on radar and satellite images at the time of the tornado do not show any evidence of the supercell character of the convection. The previous diagnosis seems to confirm that the tornado developed from a non-supercell storm. But, at this point, it is very difficult to understand the V-shape signature (McCann, 1981), probably corresponding to a supercell since it produced large hail, observed in a NOAA image (see Figure 11 in RALM), after the development of the tornado.

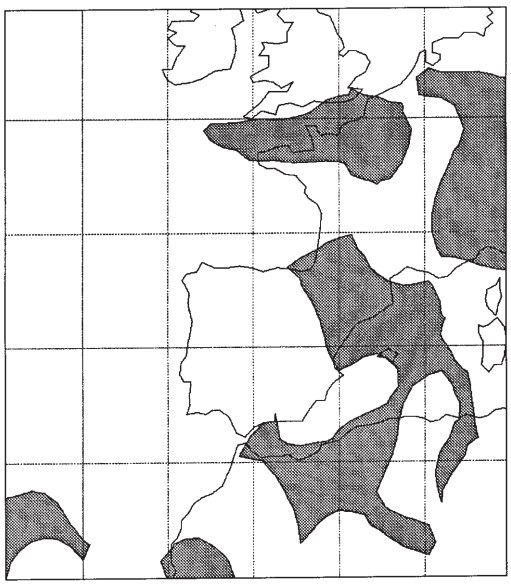

Figure 17. *Composite chart on 31 August 1994 at 1200 UTC deduced from ECMWF analyses. Shaded zones indicate overlap of quasi-geostrophic upward forcing at 850 hPa, convergence of water vapour in the 1000–850 hPa layer and convective instability between 1000 and 500 hPa.*

4.3. Mesoscale study

A next step is to look for lifting mechanisms able to develop convection in an explosive form. Figure 20 shows a hand-drawn surface mesoscale analysis for 31 August 1994 at 1500 UTC, the tornado time. A convergence line, which occurs parallel to the Spanish coast, is clearly depicted by the winds. This convergence line is produced by a low which developed over Catalonia as a consequence of the radiative heating (the sky was clear during all the morning, see Figure 22, and Figure 10 in RALM). Isotherms demonstrate the thermal character of the low over Catalonia. This convergence line, helped by the coastal orography in Catalonia (see Figure 1), can produce vertical motion able to drive the low-level parcels up to the level of free convection. However, a similar convergence line can be observed in the surface pressure analysis at 1200 UTC (not shown) and convection does not exist at that time (see Figure 10 in RALM). We have already shown that, at 1200 UTC, the composite chart indicates that Catalonia is included in the favoured area by the synoptic mechanisms, but at 500 hPa the forcing over Catalonia is downward and therefore able to suppress vertical motions. We have to look for other mechanisms that, when superimposed on the effect of the convergence line, can favour a strong convective development.

Figure 21 shows the hand-drawn analyses of the 500 and 200 hPa isobaric surface at 1200 UTC. At 500 hPa a trough is clearly depicted over Spain with a secondary trough over the southern coast of France. An anticyclonic circulation exists between both. A similar structure appears at 200 hPa with two jet streaks in the ascending part of the trough. The Meteosat images have

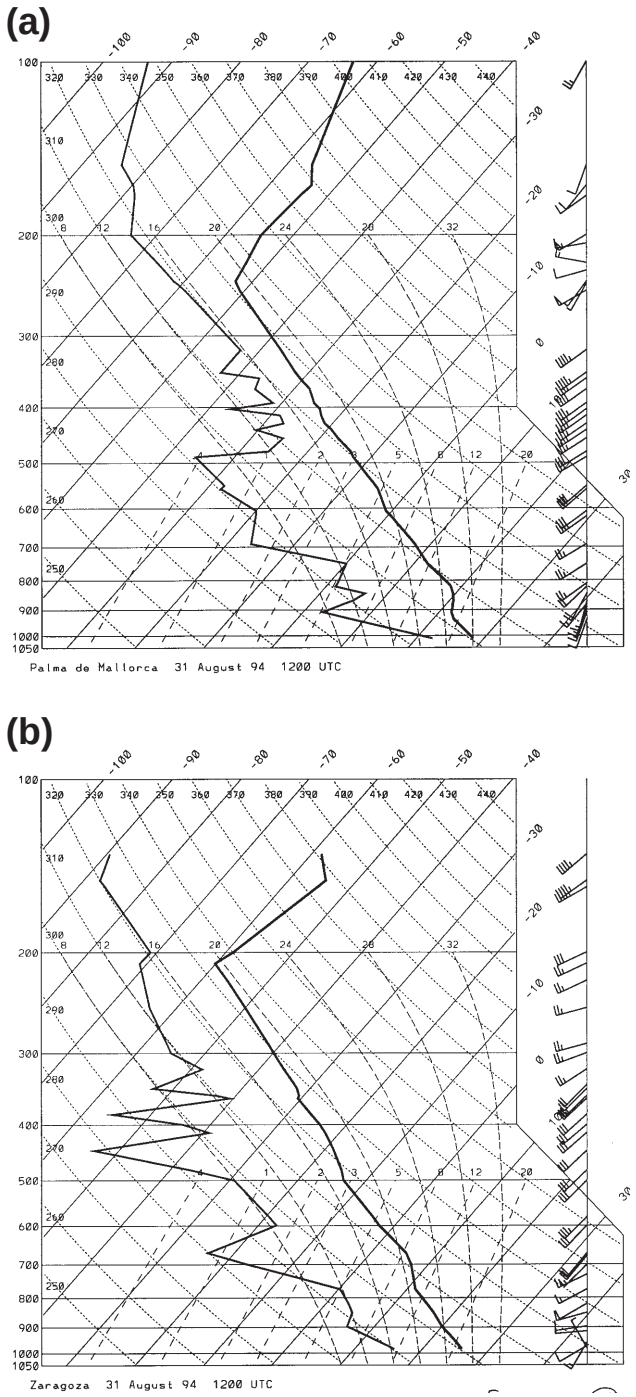

Figure 18. *Radiosoundings on 31 August 1994 at 1200 UTC for* (a) *Palma and* (b) *Zaragoza.*

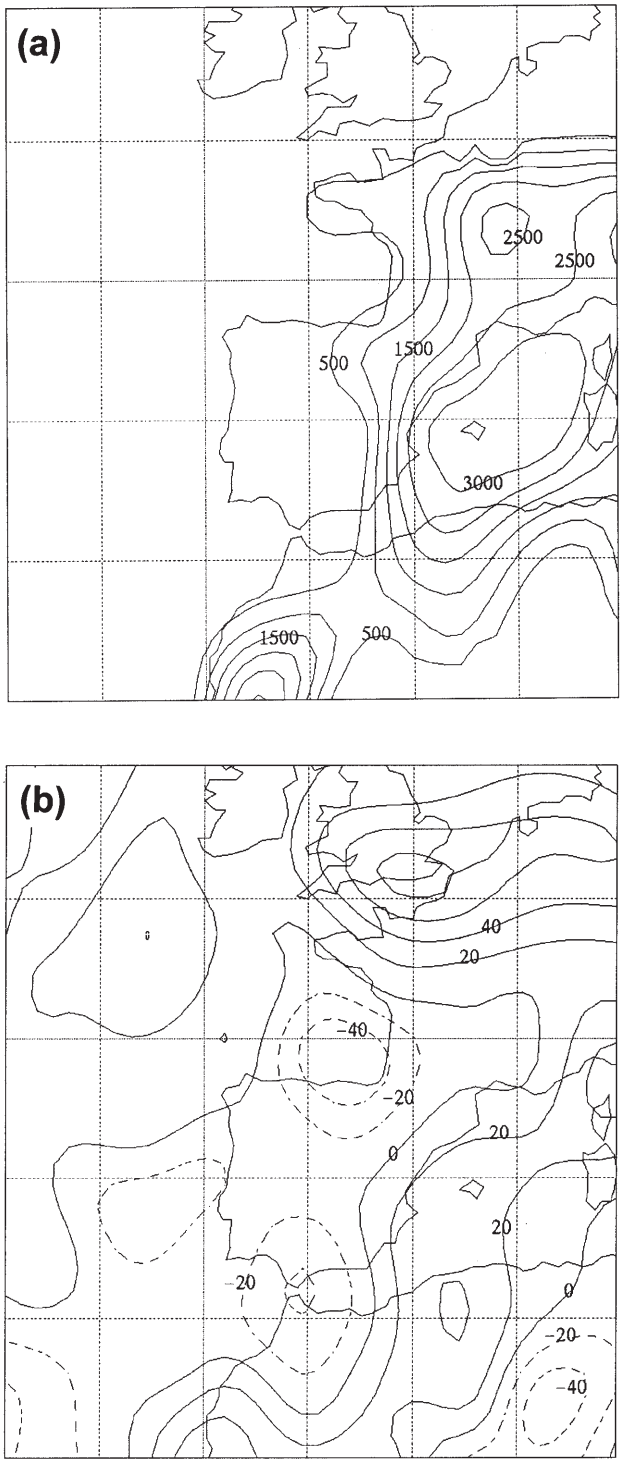

Figure 19. *Spatial distribution on 31 August 1994 at 1200 UTC, deduced from ECMWF analyses, for* (a) *CAPE (J kg^{-1}) and* (b) *Helicity (m^2 s^{-2}).*

also been used to relocate the jet streaks, previously identified on the ECMWF analysis. Figure 22 shows a band of high clouds over south-eastern Spain, which indicates the presence of a wind maximum. This cloud band can be identified in further images in such a way that it had a northern displacement and increased anticyclonic curvature (see Figure 10 in RALM). In this situation the sub-tropical jet streak over Spain and the other over France present an ideal configuration for vertical motion over Catalonia since the left exit of the Mediterranean jet interacts with the right entrance of the northern jet in this area. The combined contributions of the convergence line at low levels and the jet streak configuration at upper levels probably produced an explosive development of storms. Figure 23 shows a scheme of the elements acting at the moment of storm initiation.

More clear evidence of the vertical motion over Catalonia can be obtained through a cross-section perpendicular to the surface front. Figure 24 shows

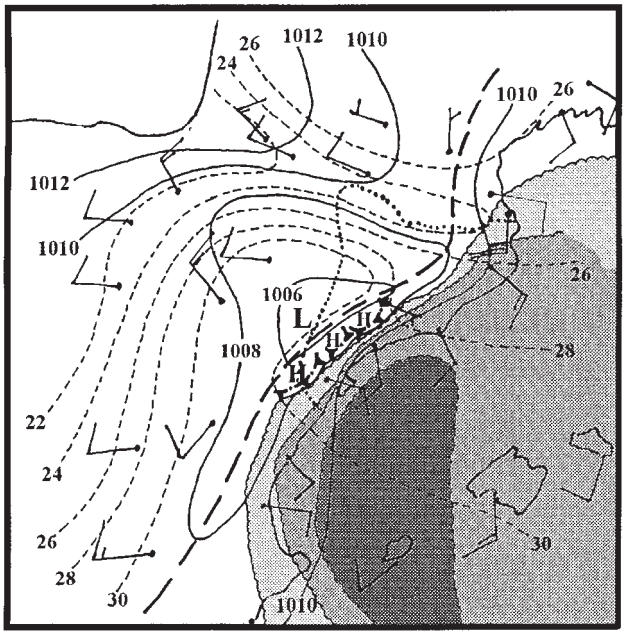

Figure 20. *Mesoscale hand-drawn surface analysis on 31 August 1994 at 1500 UTC. Full line: isobars. Dashed lines: isotherms. Shaded regions represent zones where the dew point is higher than 20, 22 and 24 °C. Winds are plotted following the conventional synoptic rules. The dotted line represents the Catalonia border.*

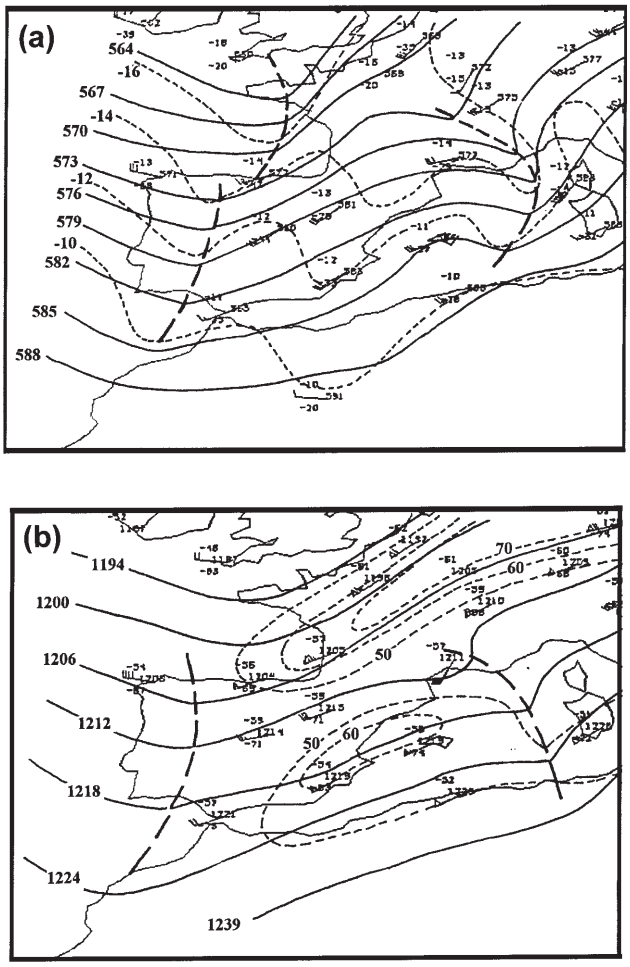

Figure 21. *Hand-drawn analyses on 31 August 1994 at 1200 UTC for* (a) *500 hPa (isohypses (full line) in damgp, isotherms (dashed) in °C) and* (b) *200 hPa (isohypses in damgp, isotachs (dashed) in kn).*

streamlines in the vertical plane by using the vertical velocity and the irrotational component of the ageostrophic wind at 1200 UTC based on ECMWF gridded data. It can be observed that the vertical circulation between the jets is upward and that it is located over Catalonia. A similar cross-section at 0600 UTC shows that upward vertical motion is located to the north-west of Catalonia, but it is weaker than at 1200 UTC.

The surface situation was slow to evolve. Figure 25 shows mesoscale analysis at 1800 UTC. The thermal low and the convergence line over have moved little since 1500 UTC. Convective cells developed along the line and affected Catalonia and southern France.

5. Comments and conclusions

The meteorological conditions associated with two cases of severe weather in north-eastern Spain have been presented. The first was produced by a squall line, with bow echo configuration in the radar echoes, that moved from west to east at a speed of 40–50 km h^{-1}, as was indicated in RALM. Strong winds, large hail and heavy rain were observed during the passage of the convective line. The second case had as the more significant event the development of a tornado with F1–F2 intensity. The development of the convection was produced explosively, and convective cells were almost stationary over Catalonia for several hours.

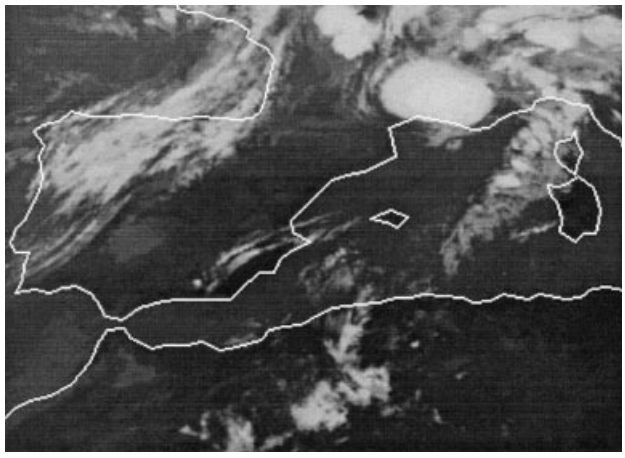

Figure 22. *Meteosat infrared image on 31 August 1994 at 0900 UTC.*

In the former case, the formation of an elevated mixed-layer inversion structure over the Ebro valley was an important ingredient. The LID formed as a consequence of the eastward displacement of warm, dry air

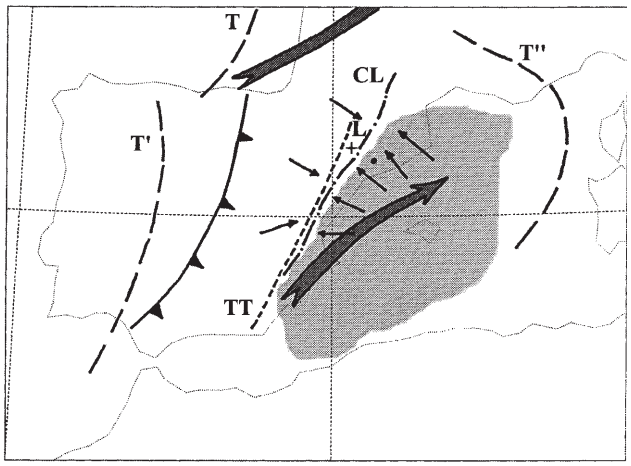

Figure 23. *Hand-drawn composite chart on 31 August 1994 at 1200 UTC showing the front and the convergence line (CL) at the surface, troughs (T, T', T'') and thermal trough (TT) at 500 hPa, and jets at 200 hPa. Full arrows represent winds at surface, and L indicates the position of the surface low and the black dot where the tornado developed. The shaded zone indicates the humid air over the Mediterranean.*

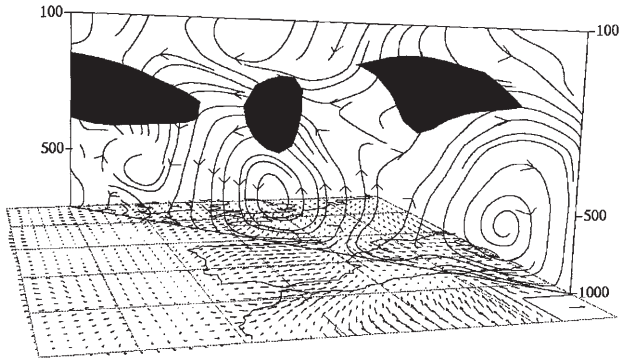

Figure 24. *Cross-section showing streamlines using vertical velocity and irrotational part of the ageostrophic wind. Black regions represent jet streaks (wind value higher than 25 m s^{-1}). Winds in the horizontal plane represent the irrotational part of the ageostrophic wind at 1000 hPa; arrow in the right corner represents 5 m s^{-1}.*

associated with the Iberian thermal low by a cyclogenetic process over Spain. The cyclogenesis occurred in response to the approach of an upper trough. The warm and dry air overran the wet and cold Mediterranean air, which penetrated a long distance inland along the Ebro valley. Large-scale circulation concentrated enough ingredients for deep convection over north-eastern Spain; in particular, quasi-geostrophic upward forcing at low levels, convergence of water vapour and convective instability. The mesoscale lifting mechanism, sufficient to break the inversion, was provided by a secondary trough and a jet streak acting together over the edge of the LID. This lifting mechanism also can explain the linear organisation of the convection. Instability, as indicated by CAPE, was not very high in the head of the Ebro valley at the diagnosis time. The instability required for

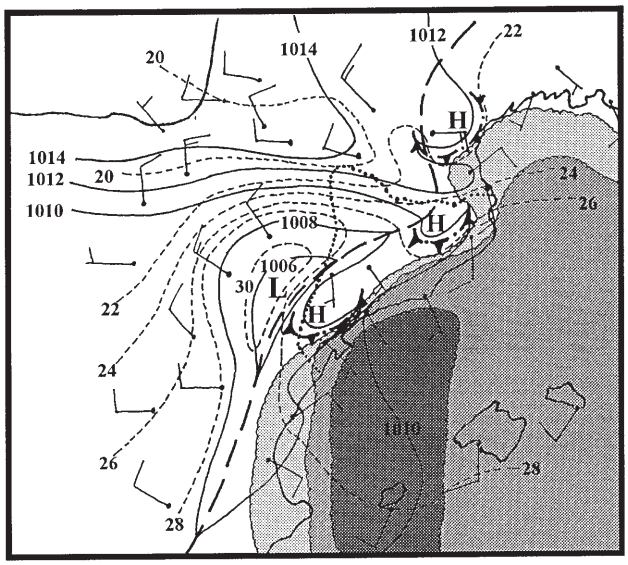

Figure 25. *As Figure 20 but at 1800 UTC on 31 August 1994.*

deep convection in that area was probably created by the warm advection at low levels and the cold air in the rear of the secondary trough when it displaced towards the north-east. Simultaneously the descending cold air associated with the secondary trough, which was moving quickly, probably provided the dry layer at medium levels needed to organise the severe convection. This fact confirms that convective environments have a great spatial and temporal variability, as is indicated by Johns & Doswell (1992), and that local conditions for instability can be created very quickly by subsynoptic systems. Once the convection developed, it moved towards the areas where the environment was more favourable. The squall line developed 150–200 km ahead of a cold front. Analysis of the thermal frontal parameter does not show clear evidence of the kata character of the front, but this possibility cannot be excluded from our diagnosis.

The meteorological conditions do not meet those identified by Johns & Hirt (1987) for the development of bow echo configurations in United States. Although the situation seems to have some similarities with the so called serial pattern, the dynamics in this case seems much weaker. Moreover Johns & Hirt (1987) do not indicate the existence of a LID in such situations. In addition the observed winds were weaker and the length of the zone affected by the winds shorter (at least over ground) than the referenced values for considering the event as a '*derecho*'. Perhaps we can call these cases '*mini-derechos*'.

From the forecaster's point of view, the most important conclusion is that the existence of a thermal low over the Iberian peninsula can represent a precedent ingredient for the development of severe weather over the eastern Spain. The formation of elevated mixed layers over the eastern Mediterranean Spanish coast has to be carefully monitored. If secondary troughs or jet streaks

can break the inversion, as the Mediterranean air is very rich in water vapour, severe weather may occur. Surface and upper-air data should be subjectively analysed and combined with a careful analysis of Meteosat images to prepare routine diagnosis of convective potential.

The tornado case represents a challenge for forecasters. On the large scale there were ingredients at low levels favourable for the convection development over Catalonia. Although quasi-geostrophic forcing at low levels was upward, the middle atmosphere opposed the upward vertical motion. The explosive development occurred when there was a combination of forcings from low levels and upper levels. At low levels a convergence line, produced by a thermal low over the coastal mountain range of Catalonia, induced upward motion. At upper levels, the mechanism was the relative position of two jet streaks such that the right entrance of one of them overlapped the left exit of the other. This positive interaction occurred also over Catalonia. It is much more difficult to identify the environment as favourable for supercell development. The CAPE is large enough but the helicity (which can be regarded as storm relative helicity, since the storms were almost stationary over Catalonia) is small. The energy–helicity index is less than 1. This fact supports the idea that the tornado was produced by a non-supercell storm, as was inferred from the radar echoes. If we accept that the environment is not favourable for supercells, it is difficult to explain a very clear V-shape signature, probably corresponding to a supercell, on a NOAA image seen some hours after the tornado development. The study of this case also shows the importance of the reanalysis of surface and upper air with the inclusion of qualitative information from Meteosat images.

The tornado developed in a valley, open to the Mediterranean Sea, in which the Francolí river runs and had a track from the south-east to the north-west (see Figure 9 in RALM). Could the orography have influenced on the development of local strong helicity at low levels when the sea breeze penetrates inland along the valley? As no meteorological information exists from the area where the tornado developed, this is only speculation. The discussion remains open but helicity enhancement by the topography has been observed previously (Hales, 1993).

Acknowledgements

This research has been partially sponsored by DGICYT of Spain under grant PB94–1169–CO2–C2. Meteorological data has been provided by the INM of Spain. We acknowledge V. Homar for his help in the graphic treatment of the data. The authors thank the Editor, Dr R Riddaway, for improve the English of the original version of the paper.

References

Alonso, S., Portela, A. & Ramis, C. (1994). First considerations on the structure and development of the Iberian thermal low-pressure system. *Ann. Geophysicae*, **12:** 457–68.

Barnes, S. L. & Newton, C. W. (1986). Thunderstorms in the synoptic setting. In *Thunderstorm Morphology and Dynamics* (Kessler, E., editor), Univ. of Oklahoma Press, 75–112.

Benjamin, S. G. & Carlson, T. N. (1986). Some effects of surface heating and the topography on the regional severe storm environment. Part I: Three-dimensional simulations. *Mon. Wea. Rev*., **114:** 307–9.

Brooks, H. E., Doswell III, C. A. & Cooper, J. (1994). On the environments of tornadic and nontornadic environments. *Wea. Forecasting*, **9:** 606–18.

Browning, K. A. (1986). Conceptual models of precipitation systems. *Wea. Forecasting,* **1:** 23–41.

Buzzi, A., Fantini, M. & Lippolis, G. (1991). Quasi-stationary organised convection in the presence of an inversion near the surface: experiments with a 2-D numerical model. *Meteorol. Atmos. Phys.*, **45:** 75–86.

Davies, J. M. (1993). Hourly helicity, instability and EHI in forecasting supercell tornadoes. *17th Conference on Severe Local Storms,* Am. Meteorol. Soc., 107–11.

Davies-Jones, R., Burgess, D. & Foster, M. (1990). Test of helicity as a tornado forecast parameter. *16th Conference on Severe Local Storms,* Am. Meteorol. Soc., 588–92.

Doswell III, C. A. (1987). The distinction between large-scale and mesoscale contribution to severe convection: a case study example. *Wea. Forecasting*, **2:** 3–16.

Doswell III, C. A. (1991). A review for forecasters on the application of hodographs to forecasting severe thunderstorms. *Nat. Wea. Digest*, **16:** 2–16.

Ducrocq, V. & Bougeault, P. (1995). Simulation of an observed squall line with a meso-beta hydrostatic model. *Wea. Forecasting*, **10:** 380–99.

Durran, D. R. & Sellman, L. W. (1987). The diagnosis of synoptic-scale vertical motion in an operational environment. *Wea. Forecasting*, **2:** 17–31.

Emanuel, K. A. (1983). On assessing local conditional symmetric instability from atmospheric soundings. *Mon. Wea. Rev*., **111:** 2016–33.

Endlich, R. M. (1967). An iterative method for altering the kinematic properties of wind fields. *J. Appl. Meteorol.,* **6:** 837–44.

Farrel, R. J. & Carlson, T. N. (1989). Evidence for the role of the Lid and Underrunning in an outbreak of tornadic thunderstorms. *Mon. Wea. Rev.*, **117:** 857–71.

Fernández, C., Gaertner, M. A., Gallardo, C. & Castro, M. (1995). Simulation of a long-lived meso-β scale convective system over the Mediterranean coast of Spain. Part I: Numerical predictability. *Meteorol. Atmos. Phys.*, **56:** 157–79.

Font, I. (1983). *Climatology of Spain and Portugal* (in Spanish). Instituto Nacional de Meteorología, Apartado 285, 28071 Madrid, 296 pp

Fujita, T. T. (1989). Tornadoes and downbursts in the context of generalized planetary scales. *J. Atmos. Sci.*, **38:** 1511–34.

Galway, J. G. (1956). The lifted index as a predictor of latent instability. *Bull. Am. Meteorol. Soc.*, **37:** 528–9.

García-Dana, F., Font R. &. Rivera, A. (1982). *Meteorological situation during the heavy rain event in the eastern zone of Spain during October-82* (in Spanish). Instituto Nacional de Meteorología, Apartado 285, 28071 Madrid, 80 pp.

Gayá, M. & Soliño, A. (1993). Tornadoes and downbursts in Menorca (in Spanish). *Rev. de Menorca*, **I:** 5–18.

Hakim, G. J. & Uccellini, L. W. (1992). Diagnosing coupled Jet Streak circulations for a northern plains snow band from the operational nested-grid model. *Wea. Forecasting*, **7:** 26–48.

Hales, J. E. Jr. (1993). Topographically induced helicity enhancement and its role in the Los Angeles basin tornado maximum. *17th Conference on Severe Local Storms. Am. Meteorol. Soc.*, 98–101.

Holton, J. R. (1993). *An Introduction to Dynamic Meteorology*. Third Edition. Academic Press. 511 pp.

Hoskins, B. J & Pedder, M. A. (1980). The diagnosis of middle latitude synoptic development. *Q. J. R. Meteorol. Soc.*, **106:** 707–19.

Johns, R. H. & Hirt, W. D. (1987). Derechos: widespread convectively induced winds. *Wea. Forecasting*, **2:** 32–49.

Johns, R. H. & Doswell III, C. A. (1992). Severe local storms forecasting. *Wea. Forecasting*, **7:** 588–612.

Johns, R. H. (1993). Meteorological conditions associated with bow echo development in convective systems. *Wea. Forecasting,* **8:** 294–9.

Llasat, M. C. (1987). *Heavy rain events in Catalonia: genesis, evolution and mechanism* (in Spanish). Ph.D. Thesis., University of Barcelona Press, 250 pp.

Maddox, R. A. (1980). Mesoscale convective complexes. *Bull. Amer. Meteorol. Soc.*, **61:** 1374–87.

Martín, F., de Esteban, L. & Riosalido, R. (1995). *The Sigüenza tornado* (in Spanish). Nota Técnica no. 25. Instituto Nacional de Meteorología, Apartado 285, 28071 Madrid, 42 pp.

McCann, D. W. (1981). *The enhanced-V, a satellite observable severe storm signature*. NOAA Technical Memorandum. NWS NSSFC-4, 31 pp.

McNulty, R. P. (1995). Severe and convective weather: a central region forecasting challenge. *Wea. Forecasting*, **10:** 187–202.

Millán, M. M. & Artiñano, B. (1992). *Mesometeorological cycles of air pollution in the Iberian peninsula.* Commission of the European Communities DG XII. Air pollution research report 44. 219 pp.

Miller, R. C. (1972). *Notes on analysis and severe storm forecasting procedures of the Air Force Global Weather Control*. AFGWC Tech. Report 200, Air Weather Service, US Air Force, 102 pp.

Miró-Granada, J. (1969). An exceptional hail event in Mallorca (in Spanish). *Rev. de la Soc. Hist. Natural de Baleares*, **XV:** 20–56.

Moller, A. R., Doswell III, C. A., Foster, M. P. & Woodall, G. R. (1994). The operational recognition of supercell thunderstorm environments and storm structures. *Wea. Forecasting*, **9:** 327–47.

Przybylinski, R. W. (1995). The bow echo: observations, numerical simulations, and severe weather detection methods. *Wea. Forecasting*, **10:** 203–18.

Ramis, C. & Alonso, S. (1992). Some considerations on the omega equation (in Spanish). *Proceedings of the I Congreso Iberoamericano de Meteorologia*, Salamanca. Spain, 117–22 (available from Asociación Meteorológica Española, Apartado 285, 28071 Madrid, Spain).

Ramis, C., Llasat, M. C., Genovés, A. & Jansà, A. (1994). The October-1987 floods in Catalonia: synoptic and mesoscale mechanism. *Meteorol. Appl.*, **1:** 337–50.

Ramis, C., Alonso, S. & Llasat, M. C. (1995). A comparative study of two cases of heavy rain in Catalonia: synoptic and mesoscale mechanisms. *Surv. Geophys.*, **16:** 141–61.

Ramis, C., Arús, J., López, J. L. & Mestre, A. (1997). Two cases of severe weather in Catalonia (Spain). An observational study. *Meteorol. Appl.*, **4:** 207–217.

Riosalido, R. (1990). Satellite characteristics of Mesoscale Convective Systems over Spain. *Proceedings of the Eighth Meteosat Scientific Users Meeting*, EUMETSAT EUMPO8, 127–30.

Rockwood, A. A. & Maddox, R. A. (1988). Mesoscale and synoptic interactions leading to intense convection: the case of 7 June 1982. *Wea. Forecasting*, **3:** 51–68.

Romero, R., Ramis, C. & Alonso, S. (1997). Numerical simulation of an extreme rainfall event in Catalonia: role of the orography and evaporation from the sea. *Q. J. R. Meteorol. Soc.*, **112:** 537–59.

Schofield, R. A. & Purdom, J. F. W. (1986). The use of satellite data for mesoscale analysis and forecasting applications. In *Mesoscale Meteorology and Forecasting* (Ray, P. S., editor), Am. Meteorol. Soc., 118–150.

Suomi, V., Fox, R., Limaye, S. & Smith, W. (1983). McIDAS III: a modern interactive data access and analysis system. *J. Appl. Meteorol.***: 22:** 766–78.

Tudurí, E. & Ramis, C. (1997). The environments of significant convective events in the western Mediterranean. *Wea. Forecasting*, **12:** 294–306.

Uccellini, L .W. (1975). A case study of apparent gravity waves initiation of severe convection storms. *Mon. Wea. Rev.,* **103:** 497–513.

Uccellini, L. W. & Johnson, D. R. (1979). The coupling of upper and lower Jet Streaks and implications for the development of severe convective storms. *Mon. Wea. Rev.*, **107:** 682–703.

Weisman, M. L. & Klemp, J. B. (1986). Characteristics of isolated convective storms. In *Mesoscale Meteorology and Forecasting* (Ray, P. S., editor). *Am. Meteorol. Soc.*, 331–58.